## ARTICLE IN PRESS

Journal of Biomechanics ■ (■■■) ■■■-■■■



Contents lists available at ScienceDirect

## Journal of Biomechanics

journal homepage: www.elsevier.com/locate/jbiomech www.JBiomech.com



# Mechanobiological simulations of prenatal joint morphogenesis

Mario Giorgi<sup>a</sup>, Alessandra Carriero<sup>a</sup>, Sandra J. Shefelbine<sup>a,b</sup>, Niamh C. Nowlan<sup>a,\*</sup>

#### ARTICLE INFO

Article history: Accepted 6 January 2014

Keywords: Joint shape Cartilage growth Chondrogenesis Computational model Joint biomechanics

#### ABSTRACT

Joint morphogenesis is the process in which prenatal joints acquire their reciprocal and interlocking shapes. Despite the clinical importance of the process, it remains unclear how joints acquire their shapes. In this study, we simulate 3D mechanobiological joint morphogenesis for which the effects of a range of movements (or lack of movement) and different initial joint shapes are explored. We propose that static hydrostatic compression inhibits cartilage growth while dynamic hydrostatic compression promotes cartilage growth. Both pre-cavitational (no muscle contractions) and post-cavitational (with muscle contractions) phases of joint development were simulated. Our results showed that for hinge type motion (planar motion from  $45^{\circ}$  to  $120^{\circ}$ ) the proximal joint surface developed a convex profile in the posterior region and the distal joint surface developed a slightly concave profile. When 3D movements from  $40^{\circ}$  to  $-40^{\circ}$  in two planes were applied, simulating a rotational movement, the proximal joint surface developed a concave profile whereas the distal joint surface rudiment acquire a rounded convex profile, showing an interlocking shape typical of a ball and socket joint. The significance of this research is that it provides new and important insights into normal and abnormal joint development, and contributes to our understanding of the mechanical factors driving very early joint morphogenesis. An enhanced understanding of how prenatal joints form is critical for developing strategies for early diagnosis and preventative treatments for congenital musculoskeletal abnormalities such as developmental dysplasia of the hip.

© 2014 The Authors. Published by Elsevier Ltd. This is an open access article under the CC BY license (http://creativecommons.org/licenses/by/3.0/).

### 1. Introduction

Joint morphogenesis is the process in which a distinct and functional joint shape starts to appear during prenatal joint development. Pacifici et al. (2005) describe the process of synovial joint formation as a well-defined sequence of three events: (1) a layer of compact and closely associated mesenchymal cells form the interzone, (2) cavitation results in the physical separation of the adjacent skeletal elements within the interzone, and (3) joint shape occurs through the process of morphogenesis. Recent studies, however, have shown that joint morphogenesis starts before cavitation (Nowlan and Sharpe, advance online publication). The consequences of incomplete or abnormal morphogenesis can be debilitating, such as in the case of developmental dysplasia of the hip (DDH) which has a frequency of 5 per 1000 hips (Bialik et al., 1999). Despite the clinical relevance of joint morphogenesis there is very little understanding about the factors that drive the process (Pacifici et al., 2005).

A small number of studies have shown that foetal immobilisation can alter joint shape development. Studies using neuromuscular blocking agents to immobilise chicks embryos have found a reduction in width of the intercondylar fossa of the distal femur and of the proximal epiphysis of the tibiotarsus and fibula during knee joint morphogenesis (Roddy et al., 2011b), and up to a 50% reduction in the epiphyseal width of the proximal and distal regions of the knee, tibiotarsus and metatarsus (Osborne et al., 2002). Mikic et al. (2000) reported morphological abnormalities including joint fusion and non-interlocking joint shapes in the post-cavitational stages of joint development. Similarly, studies of genetically modified "muscleless limb" mice have revealed changes in joint morphogenesis, particularly in the elbow and shoulder (Kahn et al., 2009; Nowlan et al., 2010). Though it is clear that lack of motion affects joint shape morphogenesis, few studies have explored the role of motion or loading on joint shape in depth.

Only one computational study has explored the role of motion on joint morphogenesis (Heegaard et al., 1999). An idealised planar biomechanical model of the proximal interphalangeal joint was used to simulate epiphyseal growth using a modified version of the endochondral ossification theory proposed by Carter et al. (1987), in which growth and shape depends on the biological

http://dx.doi.org/10.1016/j.jbiomech.2014.01.002

0021-9290 © 2014 The Authors. Published by Elsevier Ltd. This is an open access article under the CC BY license (http://creativecommons.org/licenses/by/3.0/).

Please cite this article as: Giorgi, M., et al., Mechanobiological simulations of prenatal joint morphogenesis. Journal of Biomechanics (2014), http://dx.doi.org/10.1016/j.jbiomech.2014.01.002

<sup>&</sup>lt;sup>a</sup> Department of Bioengineering, Imperial College London SW7 2AZ, UK

<sup>&</sup>lt;sup>b</sup> Department of Mechanical and Industrial Engineering, Northeastern University, USA

<sup>\*</sup> Corresponding author. Tel.: +44 0 2075945189.

E-mail address: n.nowlan@imperial.ac.uk (N.C. Nowlan).

growth (i.e. the intrinsic growth due to hormones, genes and nutrients), and mechanical growth (i.e. region-specific growth due to muscle, ligament and joint forces). The model predicted the development of congruent surfaces within the joint region and was the first mechanobiological simulation of any aspect of prenatal joint development. While the Heegaard et al. (1999) study was undeniably ground-breaking, there are a number of ways in which it can be advanced upon. Firstly, examining precavitation time-points would show the influence of static loads before motion occurs. Morphogenesis has been shown to commence prior to cavitation (Nowlan and Sharpe, advance online publication), and therefore static loading prior to cavitation may play a role in early joint shape. Secondly, experimental studies indicate that static compressive loading inhibits cartilage growth (Burton-Wurster et al., 1993; Guilak et al., 1994) while cyclic compressive loading promotes growth (Kim et al., 1994; Korver et al., 1992; Parkkinen et al., 1992), and so a mechanobiological theory specific to these properties of cartilage growth would provide a significant insight. Finally, using multiple loading conditions and longer iteration times could enable a range of realistic joint shapes to be obtained.

In this study, we propose a 3D mechanobiological simulation of joint morphogenesis in which the effects of a range of movements and different initial joint shapes are explored. Following previous studies, growth and adaptation are directed by biological and mechanobiological factors. Both pre- and post-cavitational phases of joint development are simulated, representing static and dynamic loading phases respectively. Prior to the onset of spontaneous muscle contracts in the limb, we assume that precavitational joints experience static loading due to growth related strains (Henderson and Carter, 2002). We use idealised shapes to represent a generic ball and socket joint and a generic hinge joint, and apply movement patterns typical for these joints in order to predict the effects on shape development. We also examine the effect of rigid paralysis on joint shape by growing a joint when no movement is applied.

#### 2. Methods

#### 2.1. Model geometry and material properties

Three idealised geometries of common joint configurations were created in Abaqus (Dassault Systemes, CAE module, version 6.12), where all configurations consisted of two opposing cartilage rudiments and a synovial capsule. A hinge joint configuration was composed of two cylindrical rudiments of the same dimensions

with hemispherical opposing ends, with the distal rudiment at an initial angle of  $45^{\circ}$  to the vertical proximal rudiment, as shown in Fig. 1-A. A ball-and-socket configuration was composed of a distal cylindrical rudiment opposed to a flat proximal rudiment representing a bone such as the pelvis or shoulder, as shown in Fig. 1-B. A similar configuration to the hinge was used for the rigid paralysis configuration, except that the two rudiments were aligned, as shown in Fig. 1-C. As these configurations are intended to be generic and not to be representative of any particular species or animal, the initial dimensions (as shown in Fig. 1) were arbitrary, and size changes due to growth or adaptation were analysed as relative to the initial size. For the purposes of performing sensitivity analyses, 2D versions of the 3D models were used. The 2D models predicted the same geometrical changes as a midline longitudinal section of the 3D versions for the range of loading regimes.

The synovial capsule was modelled as a sphere surrounding the joint, (truncated at its extremes in order to decrease the number of elements) with a maximal diameter of 10 mm and large enough to contain the joint throughout movement sequences (Fig. 1-D). In order to quantify the effects of inclusion of the synovial capsule, 2D hinge simulations were run both with and without the capsule. Based on the stage of joint development being modelled, the rudiments were assumed to be fully cartilaginous (Gardner and O'Rahilly, 1968). All cartilage material properties were assumed to be linear elastic, isotropic and homogeneous. The Young's modulus for cartilage (E=1.1 MPa) was taken from four-point bending tests on un-mineralised embryonic mouse ribs (Tanck et al., 2004) and the cartilage Poisson's ratio taken as  $\nu$ =0.49 to reflect the incompressibility of the fluid in the cartilage at short time scales (Armstrong et al., 1984; Carter and Beaupré, 1999; Wong et al., 2000). The Young's modulus of the synovial capsule was E=0.287 kPa (Roddy et al., 2011a), and its Poisson's ratio was  $\nu$ =0.4 (McCarty et al., 2011).

#### 2.2. Loading conditions

In all models, the proximal rudiment was fixed at its proximal end. At rest, the bottom rudiment was located 0.2 mm from the top rudiment's lower surface (Fig. 1). Static and dynamic loading were represented by an applied displacement of the distal rudiment towards the proximal (upper fixed) rudiment. In the precavitational phase, prior to the onset of muscle contractions, static loading due to growth-related strains (Henderson and Carter, 2002) was represented by the constant application of an axial displacement on the distal rudiment towards the proximal rudiment in the starting configuration. In the post-cavitational phase, after the onset of muscle contractions, joint loads were represented by a number of steps during which a displacement was applied to the lower surface of the distal rudiment towards the proximal element, with the angle and position of the displacement determined by the type of movement being applied. The magnitude of the displacement applied, 10  $\mu$ m, remained constant throughout all simulations. Based on approximations of muscle cross sectional area (as a percentage of rudiment width) and allowable maximum embryonic muscle stress of S=1.11 mN/mm<sup>2</sup> (Nowlan et al., 2008), we estimated the likely muscle force to be on the order of 0.1 mN. An applied displacement of 10  $\mu m$  resulted in a force of approximately this magnitude. In the absence of data on the magnitude of growth related strains in the developing joint, the same displacement was used for the static phase. Two static iterations (pre-cavitation with no motion) and eight dynamic iterations (post-cavitation with motion) were included in the hinge and ball-and-socket simulations. In the hinge model, a single plane motion was applied from  $45^{\circ}$  to  $120^{\circ}$  in each iteration, as shown in Fig. 1-A, at angles of  $45^{\circ}$ ,  $90^{\circ}$  and  $120^{\circ}$ , while the ball-and-socket model was loaded under a multi-plane motion

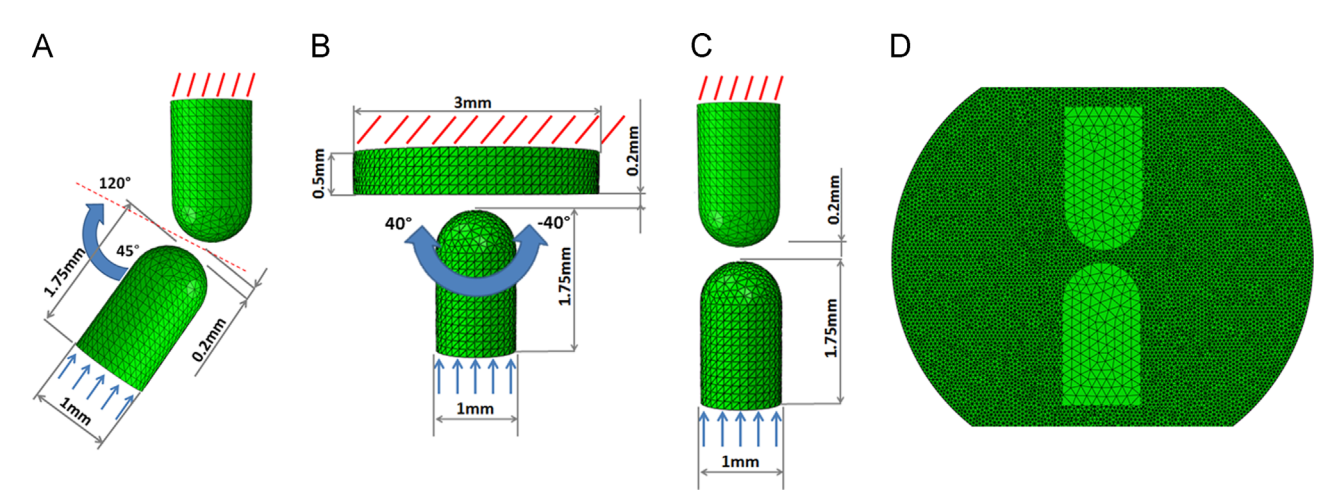


**Fig. 1.** Configuration of the models. (A) Hinge model configuration, with the initial rudiment at an initial angle of 45° to the vertical proximal rudiment. (B) Ball-and-socket configuration with a distal cylindrical rudiment opposed to a flat proximal rudiment. (C) Rigid paralysis configuration, the two rudiments are aligned along their vertical axis. (D) Section of the rigid paralysis configuration with synovial capsule.

from  $40^\circ$  to  $0^\circ$  to  $-40^\circ$  in two planes perpendicular to each other as shown in Fig. 1-B. Rigid paralysis, where the muscles are in continuous tetanus (Roddy et al., 2011b) was represented by the constant application of an axial displacement, as shown in Fig. 1-C, assumed to be static loading due to the lack of dynamic muscle contractions. The paralysis model was also run in 2D with the distal rudiment at  $-60^\circ$  to the proximal rudiment. Frictionless impenetrable contact was modelled between all the components of the models.

#### 2.3. Growth rate

Growth and morphogenesis of the rudiments were controlled by biological and mechanical growth rates so that the growth rate  $d\varepsilon/dt$  was as follows:

$$\frac{d\varepsilon}{dt} = \frac{d(\varepsilon_b)}{dt} + \frac{d(\varepsilon_m)}{dt}$$

with  $\dot{e}_b$  the biological contribution to growth and  $\dot{e}_m$  the mechanical contribution to growth (Shefelbine and Carter, 2004). Following Heegaard et al. (1999),  $\dot{e}_b$  was considered to be proportional to the chondrocyte density. The equation for local chondrocyte density along the long axis of a rudiment was calculated by Heegaard et al. (1999) by fitting a polynomial curve to the grey level distribution on a sagittal micrograph of a joint, where darker areas indicated higher chondrocyte density. The chondrocyte density  $C_d$  is greater towards the ends of the rudiments and lower towards the diaphysis, and therefore expressed by the formula

$$\dot{\varepsilon}_b = C_d = k(0.14 - 0.87\xi + 4.40\xi^2 - 2.66\xi^3)$$

with  $C_d$  being the chondrocyte density,  $k{=}11 \times 10^3$  being a constant determining the amount of biological growth, which is maintained in the range of 75–85% of the total growth (Germiller and Goldstein, 1997), and  $\xi$  the distance along the proximal-distal axis of the rudiment starting from the distal end (Heegaard et al., 1999). The biological contribution to growth was assumed to be constant during static and dynamic loading phases. The effects of alternative equations for the chondrocyte density were also analysed in 2D versions of the hinge simulation.

The mechanical growth rate,  $\dot{\epsilon}_m$ , was proportional to the compressive hydrostatic stress,  $\sigma_h$ . Previous experimental studies have found that static compression significantly inhibits the synthesis of cartilage matrix proteins (Burton-Wurster et al., 1993; Guilak et al., 1994) while dynamic compression stimulates matrix production (Kim et al., 1994; Korver et al., 1992; Parkkinen et al., 1992). Accordingly, we implemented a mechanobiological theory in which static hydrostatic compression inhibits cartilage growth while dynamic hydrostatic compression promotes cartilage growth. The mechanobiological growth rate was also considered to be proportional to the chondrocyte density, based on the assumption that the greater the number of cells, the greater the adaptation to mechanical loading. The overall mechanobiological contribution to growth was therefore calculated at each node of the model as the average stresses throughout a full joint motion using the formulae

helow

$$\dot{\varepsilon}_m = C_d \left( \frac{\sum\limits_{i=1}^N \sigma_{hi}}{N} \right)$$
, for static loads

$$\dot{\varepsilon}_m = -C_d \left( \frac{\sum\limits_{i=1}^N \sigma_{hi}}{N} \right)$$
, for dynamic loads

where  $\sigma_h$  is the compressive hydrostatic stress, N the number of movement per step and  $C_d$  the chondrocyte density.

#### 2.4. Model implementation

During each iteration, the orthonormal thermal expansion capabilities of the FE solver were utilised to allow isotropic expansion of the proximal and distal rudiments with the sum of the biological and mechanobiological growth rates used as the 'temperature' for expansion. This expansion occurred within an unconstrained volume, representing the growth of the entire limb, which ensured that the mechanical stresses due to motion were the dominant stimulus for shape change rather than stresses due to contact of the two rudiments during growth. The new geometry was then re-meshed and the two rudiments were automatically realigned, so that the loading conditions could be applied again for another step of growth. The size and shape of the synovial capsule remained the same for the entire simulation. A simulation using biological growth rates only was also performed for comparative purposes.

#### 3. Results

#### 3.1. Hydrostatic stress distribution

In all the models, the hydrostatic stresses close to the contact regions were always compressive, as shown in Fig. 2. High compressive hydrostatic stresses were also seen at the anterior corner of the proximal rudiment of the hinge model due to the fixed boundary condition (Fig. 2, arrows). The simulation in which rigid paralysis was modelled induced a symmetric stress pattern on the rudiments, as shown in the first (static) phase of the hinge simulation (Fig. 2, left).

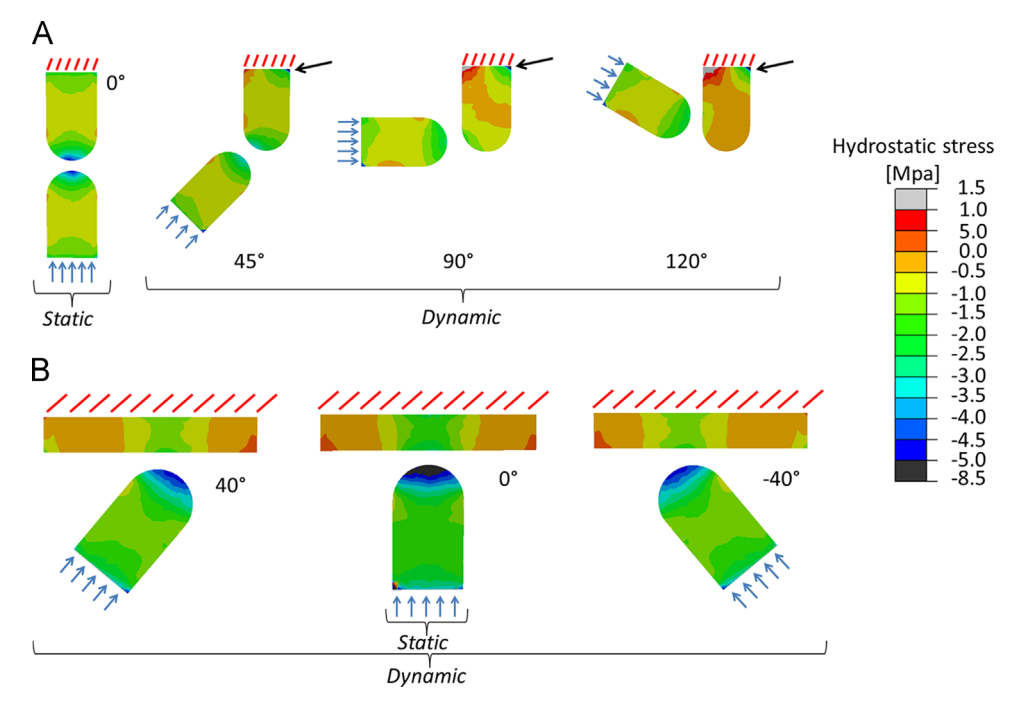


Fig. 2. Hydrostatic stress distribution during the first step of static and dynamic loading for the (A) hinge and the (B) ball-and-socket joint, respectively. In both joint models, the highest hydrostatic compression stresses are seen within the region of contact between the two rudiments.

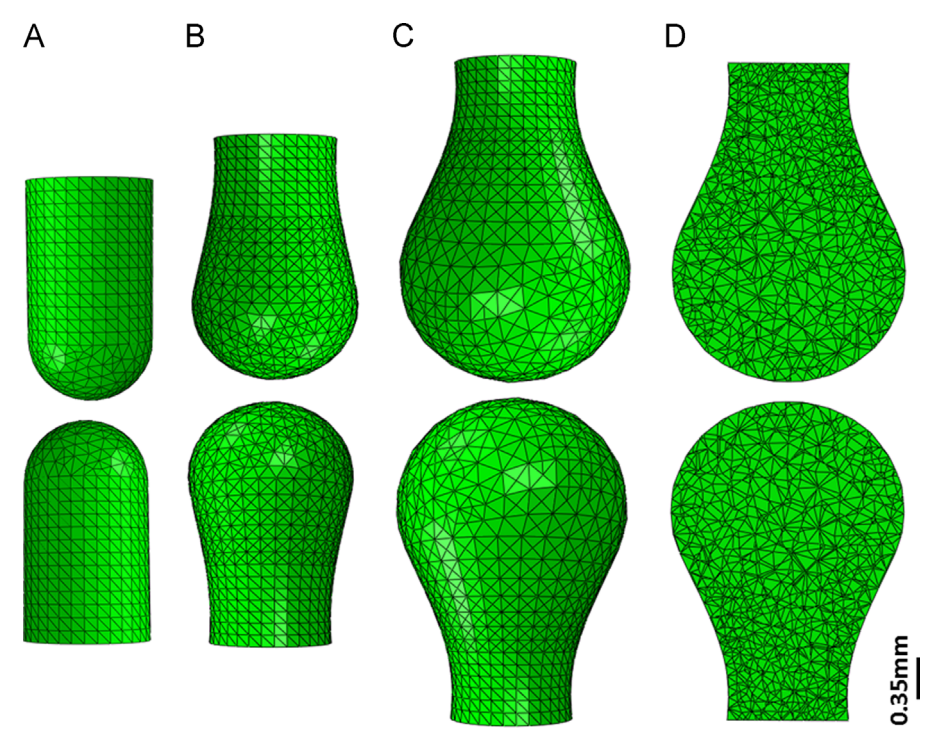


Fig. 3. Joint morphogenesis prediction when only the biological contribution to growth was considered. (A) Sagittal view of the initial model. (B) Sagittal view of the predicted joint shape after 10 steps of growth. (D) Sagittal section after 10 steps of growth. Scale bar = 0.35 mm.

### 3.2. Morphogenesis

When biological growth alone was applied, the rudiments preserved their initial opposing convex surfaces as shown in Fig. 3. In contrast, when the mechanical stimulus was included in the simulation, the shape of the predicted growing joints changed according to the movement pattern applied. When a single plane motion from 45° to 120° was applied, the proximal rudiment showed a rounded convex profile in both posterior and anterior regions, with more pronounced growth posteriorly (Fig. 4, arrowhead). The distal rudiment showed similar features with a less pronounced rounded convex profile in its posterior region and the acquisition of a slight concave profile in the mid-line section (Fig. 4, arrow). When a multi-plane motion from  $40^{\circ}$  to  $-40^{\circ}$ degrees was applied between a flat and a cylindrical rudiment, the flat rudiment showed a concave profile which partially enclosed the rounded convex profile of the cylindrical rudiment (Fig. 5). When only axial forces were applied under static loading conditions, reproducing rigid paralysis, both the rudiments acquired a flat shape within the joint region as shown in Fig. 6, similar to the experimental results of Mikic et al. (2000). Flat opposing surfaces were also predicted when the same simulation was run in 2D with the distal rudiment at  $-60^{\circ}$  to the proximal rudiment (data not shown).

#### 3.3. Sensitivity analyses

When simulations were run without a synovial capsule, small differences in shape were found due to stress concentrations at the contact regions, but similar patterns of growth for the models with and without synovial capsule were predicted. Similarly, when a linear approximation of the polynomial equation for chondrocyte density was used there was no major effect on joint shape or growth. Analysis of the effects of varying the relative influence of the biological and mechanobiological contributions demonstrated that with a higher biological contribution, the mechanobiological contribution was too low to have an influence on the total growth

and joint morphology. With a lower weighting for the biological contribution, the effects of the mechanobiological stimulus were more evident with more extreme changes at the epiphyses and decreased growth overall (data not shown for sensitivity analyses).

#### 4. Discussion

We have developed the first 3D mechanobiological models of prenatal joint shape development, which are capable of predicting a range of joint shapes based on the starting joint configuration and applied movements.

When a hinge movement from  $45^{\circ}$  to  $120^{\circ}$  was applied, the proximal rudiment acquired a rounded convex profile in its posterior and anterior regions with a more pronounced growth posteriorly, and the distal rudiment acquired a slight concave profile in the middle, as shown in Fig. 4, suggesting the generation of an interlocking joint shape such as the knee. When a rotational movement from  $40^{\circ}$  to  $-40^{\circ}$  was applied, the proximal rudiment developed a clear concave profile in which the rounded convex profile of the distal rudiment was contained at its proximal end, as shown in Fig. 5, suggesting the generation of an interlocking joint shape such as the hip or shoulder joint. When only axial forces were applied under static loading conditions, reproducing rigid paralysis, both the rudiments acquired a flat shape within the joint region (Fig. 6) similar to the experimental results of Mikic et al. (2000) for the immobilised interphalangeal joint.

Based on recent evidence that joint shape initiates prior to cavitation (Nowlan and Sharpe, advance online publication), we have modelled the development of the joint under both static and dynamic loads, characteristic of pre- and post- cavitation, respectively. We have developed a novel mechanobiology theory of cartilage growth, based on experimental evidence from *in vitro* stimulation of chondrocytes (Burton-Wurster et al., 1993; Guilak et al., 1994; Kim et al., 1994; Korver et al., 1992; Parkkinen et al., 1992). Despite the abundance of mechanobiological theories and mechanobiological simulations relating to endochondral

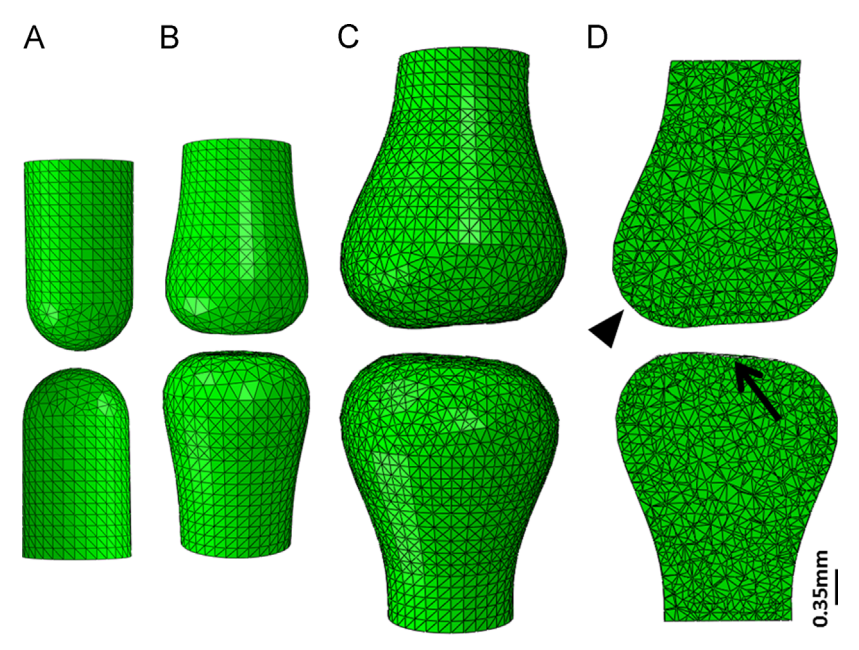


Fig. 4. Joint morphogenesis prediction when a single plane motion from 45° to 120° is applied. (A) Sagittal view of the initial model. (B) Sagittal view of the predicted joint shape after 2 static steps of growth. (C) Sagittal view of the predicted joint shape after 2 static and 8 dynamic steps of growth. (D) Sagittal section after 2 static+8 dynamic steps of growth. Scale bar=0.35 mm.

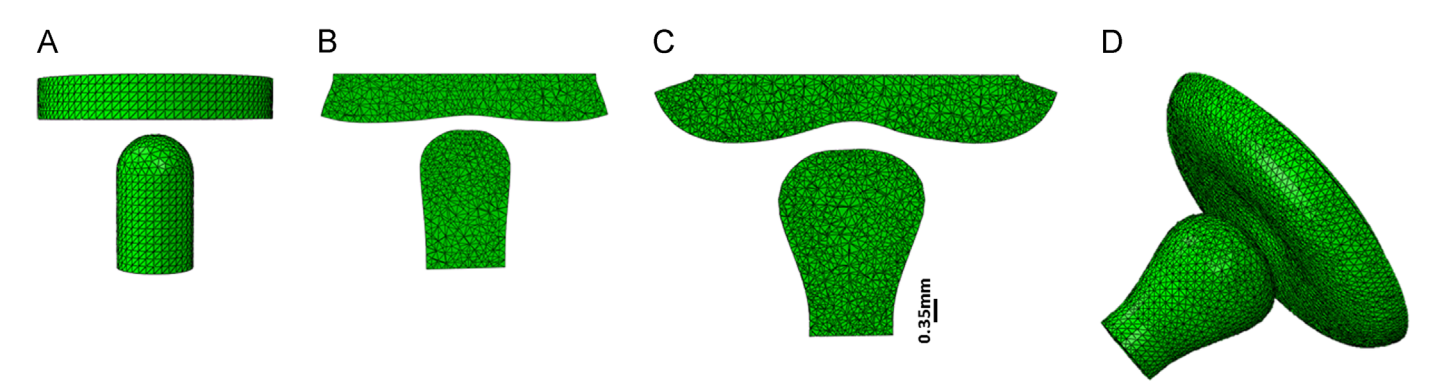


Fig. 5. Joint morphogenesis prediction when a multi plane motion from  $40^{\circ}$  to  $-40^{\circ}$  is applied. (A) Sagittal view of the initial model. (B) Sagittal section of the predicted joint shape after 2 static steps of growth. (C) Sagittal section of the predicted joint shape after 2 static and 8 dynamic steps of growth. (D) Rotated view after 2 static+8 dynamic steps of growth. Scale bar=0.35 mm.

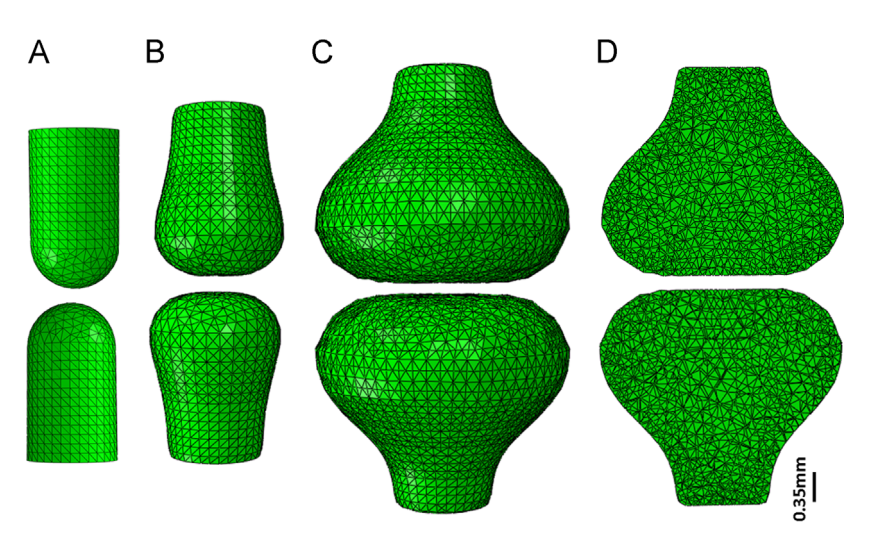


Fig. 6. Joint morphogenesis when the rigid paralysis was simulated. (A) Sagittal view of the initial model. (B) Sagittal view of the predicted joint shape after 2 static steps of growth. (C) Sagittal view of the predicted joint shape after 10 static steps of growth. (D) Sagittal section after 10 static steps of growth. Scale bar=0.35 mm.

Please cite this article as: Giorgi, M., et al., Mechanobiological simulations of prenatal joint morphogenesis. Journal of Biomechanics (2014), http://dx.doi.org/10.1016/j.jbiomech.2014.01.002

ossification (Carter et al., 1998; Claes and Heigele, 1999; Huiskes et al., 1997; Lacroix and Prendergast, 2002; Lacroix et al., 2002; Prendergast et al., 1997; Sarin and Carter, 2000; Stevens et al., 1999), we are unaware of any mechanoregulation algorithm specific to cartilage growth in a non-endochondral ossification context. The growth law proposed by Heegaard et al. (1999) was based upon a theory developed for endochondral ossification (Carter et al., 1987), where hydrostatic compressive stress inhibits and tensile stress promotes cartilage growth and ossification. In contrast, our simulations focus specifically on joint epiphyses which are entirely cartilaginous at the stages modelled (Gardner and O'Rahilly, 1968), and it is likely that the mechanical stimuli for growth and adaptation of epiphyseal cartilage are different than those which influence endochondral growth and ossification. These two processes are biologically distinct, as growth at the growth plate is primarily due to chondrocyte hypertrophy (Kronenberg, 2003), while cartilage growth at the epiphysis is likely due to cell proliferation (Pacifici et al., 2005). Therefore, the mechanobiological growth law proposed here is specific to epiphyseal cartilage and is based upon experimental data showing that cyclic hydrostatic compression stimulates matrix production (Kim et al., 1994; Korver et al., 1992; Parkkinen et al., 1992) and static compression inhibits the synthesis of cartilage matrix proteins (Burton-Wurster et al., 1993; Guilak et al., 1994). However, the new theory which we propose in not in conflict with the theories previously proposed for growth plate cartilage, as in both cases, compression provides a favourable environment for cartilage. In endochondral ossification, hydrostatic compression maintains the cartilage at the growth plate, while during epiphyseal cartilage growth, hydrostatic compression promotes the formation of more cartilage. This new theory for cartilaginous joint morphogenesis differentiates between static and dynamic loading conditions, where static compressive loading inhibits cartilage growth while dynamic compressive loading promotes it. In proposing a mechanobiological theory for epiphyseal cartilage growth and adaptation, we offer a biomechanical understanding of the influence of mechanical loading on joint morphogenesis.

Material properties of synovial capsule and cartilage were assumed to be linear elastic, isotropic and homogeneous. Although cartilage is a biphasic material (Roddy et al., 2011a), and the synovial capsule is also likely to be the same (Roddy et al., 2011a), we modelled our cartilage as single phase and near incompressible (Poisson's ratio of 0.49), based on previous studies which showed that the fluid pressure in biphasic models is comparable to the hydrostatic stress in the single phase models when loaded at frequencies of 1 Hz (Carter and Wong, 2003; Shefelbine and Carter, 2004), which is close to the frequency of muscle contraction in utero (Vaal et al., 2000) Muscles and ligaments were not explicitly modelled as acting at specific location of the rudiment. However, since our models are of generic joint shapes and configurations, and do not apply to one specific species (or even limb) we focussed on the joint motion likely to result from approximations of common movement sequences.

In conclusion, this study presents how stresses generated during static growth-related loading and dynamic post-cavitational movements can influence prenatal joint morphogenesis. This study predicts joint shape morphogenesis in 3D using a novel mechanobiology theory for cartilage growth. Our simulations predict a range of anatomically recognisable joint shapes based on the starting joint configuration and applied movement. The significance of this research is that it provides new and important insights into normal and abnormal joint development. Understanding the factors driving joint morphogenesis at a very early stage is critical for developing strategies for early diagnosis and preventative treatments for congenital musculoskeletal abnormalities, such as developmental dysplasia of the hip.

#### **Conflict of interest**

The authors have no conflicts of interests relating to this research.

#### Acknowledgements

This research was funded by a Departmental Studentship from the Department of Bioengineering at Imperial College London.

#### References

- Armstrong, C.G., Lai, W.M., Mow, V.C., 1984. An analysis of the unconfined compression of articular cartilage. J. Biomech. Eng. 106, 165–173.
- Bialik, V., Bialik, G.M., Blazer, S., Sujov, P., Wiener, F., Berant, M., 1999. Developmental dysplasia of the hip: a new approach to incidence. Pediatrics 103, 93–99.
- Burton-Wurster, N., Farquhar, V.-S.M., Lust G., T., 1993. Effect of compressive loading and unloading on the synthesis of total protein, proteoglycan, and fibronectin by canine cartilage explants. J. Orthop. Res. 11, 717–729.
- Carter, D., Orr, T., Fyhrie, D., Schurman, D., 1987. Influences of mechanical stress on prenatal and postnatal skeletal development. Clin. Orthop. Relat 15, 237–250.
- Carter, D., Wong, M., 2003. Modelling cartilage mechanobiology. R. Soc. 358, 1461–1471.
- Carter, D.R., Beaupré, G.S., 1999. Linear elastic and poroelastic models of cartilage can produce comparable stress results: a comment on Tanck et al. J. Biomech. 32, 153–161.
- Carter, D.R., Beaupré, G.S., Giori, N.J., Helms, J.A., 1998. Mechanobiology of skeletal regeneration. Clin. Orthop. Relat. Res. 355, S41–S55.
- Claes, L.E., Heigele, C.A., 1999. Magnitudes of local stress and strain along bony surfaces predict the course and type of fracture healing. J. Biomech. 32, 255–266.
- Gardner, E., O'Rahilly, R., 1968. The early development of the knee joint in staged human embryos. J. Anat. 102, 289–299.
- Germiller, J.A., Goldstein, S.A., 1997. Structure and function of embryonic growth plate in the absence of functioning skeletal muscle. J. Orthop. Res. 15, 362–370.
- Guilak, F., Meyer, B.C., Ratcliffe, A., Mow, V.C., 1994. The effects of matrix compression on proteoglycan metabolism in articular cartilage explants. Osteoarthr. Cartil. 2, 91–101.
- Heegaard, J.H., Beaupré, G.S., Carter, D.R., 1999. Mechanically modulated cartilage growth may regulate joint surface morphogenesis. J. Orthop. Res. 17, 509–517.
- Henderson, J.H., Carter, D.R., 2002. Mechanical induction in limb morphogenesis: the role of growth-generated strains and pressures. Bone 31, 645–653. Huiskes, R., Driel, W.D.V., Prendergast, P.J., SØBalle, K., 1997. A biomechanical
- regulatory model for periprosthetic fibrous-tissue differentiation. J. Mater. Sci.: Mater. Med. 8, 785–788.
- Kahn, J., Shwartz, Y., Blitz, E., Krief, S., Sharir, A., Breitel, D.A., Rattenbach, R., Relaix, F., Maire, P., Rountree, R.B., Kingsley, D.M., Zelzer, E., 2009. Muscle contraction is necessary to maintain joint progenitor cell fate. Dev. Cell 16, 734–743.
- Kim, Y.J., Sah, R.L.Y., Grodzinsky, A.J., Plaas, A.H.K., Sandy, J.D., 1994. Mechanical regulation of cartilage biosynthetic behavior: physical stimuli. Arch. Biochem. Biophys. 311, 1–12.
- Korver, T.H., Van de Stadt, R.J., Kiljan, E., Van Kampen, G.P., Van der Korst, J.K., 1992.
  Effects of loading on the synthesis of proteoglycans in different layers of anatomically intact articular cartilage in vitro. J. Rheumatol. 19, 905–912.
- Kronenberg, H.M., 2003. Developmental regulation of the growth plate. Nature.
- Lacroix, D., Prendergast, P.J., 2002. A mechano-regulation model for tissue differentiation during fracture healing: analysis of gap size and loading. J. Biomech. 35, 1163–1171.
- Lacroix, D., Prendergast, P.J., Li, G., Marsh, D., 2002. Biomechanical model to simulate tissue differentiation and bone regeneration: application to fracture healing. Med. Biol. Eng. Comput. 40, 14–21.
- McCarty, W.J., Masuda, K., Sah, R.L., 2011. Fluid movement and joint capsule strains due to flexion in rabbit knees. J. Biomech. 44, 2761–2767.
- Mikic, B., Wong, M., Chiquet, M., Hunziker, E.B., 2000. Mechanical modulation of tenascin-C and collagen-XII expression during avian synovial joint formation. J. Orthop. Res. 18, 406–415.
- Nowlan, N.C., Bourdon, C., Dumas, G., Tajbakhsh, S., Prendergast, P.J., Murphy, P., 2010. Developing bones are differentially affected by compromised skeletal muscle formation. Bone 46, 1275–1285.
- Nowlan, N.C., Murphy, P., Prendergast, P.J., 2008. A dynamic pattern of mechanical stimulation promotes ossification in avian embryonic long bones. J. Biomech. 41, 249–258.
- Nowlan, N.C., Sharpe, J., Joint shape morphogenesis precedes cavitation of the developing hip joint. J. Anat, http://dx.doi.org/10.1111/joa.12143, in press.
- Osborne, A.C., Lamb, K.J., Lewthwaite, J.C., Dowthwaite, G.P., Pitsillides, A.A., 2002. Short-term rigid and flaccid paralyses diminish growth of embryonic chick limbs and abrogate joint cavity formation but differentially preserve precavitated joints. J. Musculoskelet. Neuronal Interact. 2, 448–456.

- Pacifici, M., Koyama, E., Iwamoto, M., 2005. Mechanisms of synovial joint and articular cartilage formation: recent advances, but many lingering mysteries. Birth Defects Res. Part C: Embryo Today: Rev. 75, 237–248.
- Parkkinen, J.J., Lammi, M.J., Helminen, H.J., Tammi, M., 1992. Local stimulation of proteoglycan synthesis in articular cartilage explants by dynamic compression in vitro. J. Orthop. Res. 10, 610–620.
- Prendergast, P.J., Huiskes, R., Søballe, K., 1997. Biophysical stimuli on cells during tissue differentiation at implant interfaces. J. Biomech. 30, 539–548.
- Roddy, K.A., Kelly, G.M., van Es, M.H., Murphy, P., Prendergast, P.J., 2011a. Dynamic patterns of mechanical stimulation co-localise with growth and cell proliferation during morphogenesis in the avian embryonic knee joint. J. Biomech. 44, 143–149.
- Roddy, K.A., Prendergast, P.J., Murphy, P., 2011b. Mechanical influences on morphogenesis of the knee joint revealed through morphological, molecular and computational analysis of immobilised embryos. PLoS ONE 6, e17526.

- Sarin, V.K., Carter, D.R., 2000. Mechanobiology and joint conformity regulate endochondral ossification of sesamoids. J. Orthop. Res. 18, 706–712.
- Shefelbine, S.J., Carter, D.R., 2004. Mechanobiological predictions of growth front morphology in developmental hip dysplasia. J. Orthop. Res. 22, 346–352.
- Stevens, S.S., Beaupré, G.S., Carter, D.R., 1999. Computer model of endochondral growth and ossification in long bones: biological and mechanobiological influences. J. Orthop. Res. 17, 646–653.
- Tanck, E., Van Donkelaar, C.C., Jepsen, K.J., Goldstein, S.A., Weinans, H., Burger, E.H., Huiskes, R., 2004. The mechanical consequences of mineralization in embryonic bone. Bone 35, 186–190.
- Vaal, J., van Soest, A.J.K., Hopkins, B., 2000. Spontaneous kicking behavior in infants: age-related effects of unilateral weighting. Dev. Psychobiol. 36, 111–122.
- Wong, M., Ponticiello, M., Kovanen, V., Jurvelin, J.S., 2000. Volumetric changes of articular cartilage during stress relaxation in unconfined compression. J. Biomech. 33, 1049–1054.